Study of Axes Rotation during Simple Shear Tests on Aluminum Sheets

L. Duchêne [1], B. Diouf [1], T. Lelotte [1], P. Flores [1], S. Bouvier [2], A.M. Habraken [1]

1. ArGEnCo Dept., University of Liège, Chemin des Chevreuils 1, 4000 Liege, Belgium.
2. LPMTM-CNRS UPR9001, University Paris 13, 99 av. J.B. Clément, 93200, Villetaneuse, France.

Abstract. In order to model accurately the anisotropic material behavior during finite element simulations, a precise description of the material yield locus is required. Beside the shape (linked to the material model used), the size (related to the isotropic hardening) and the position (kinematic hardening) of the yield locus, its orientation is of particular interest when large rotations of the material are encountered during the simulations. This paper proposes three distinct methods for the determination of the material yield locus rotation: a method based on the Constant Symmetric Local Velocity Gradient (CSLVG), a corotational method and a method based on the Mandel spin. These methods are compared during simple shear tests of an aluminum sheet.

Keywords: Finite element method, Simple shear test, Texture analysis, Reference frames.

INTRODUCTION

For the finite element (FE) simulations relying on elasto-plastic models based on anisotropic yield locus description, it is important for the simulation accuracy to follow a Cartesian reference frame, where the yield locus is expressed. The classical formulations like the Hill 1948 model keep a constant shape of the yield locus when more sophisticated yield loci, e.g. based on texture, regularly update their shape. However in all these cases, the rotation of the Cartesian reference frame should be known.

In large strain FE simulations, different reference frames can be defined as shown in Figure 1 for the case of a shear test. The *global frame* $\{X_1,X_2,X_3\}$ remains fixed during the whole simulation and is used to define the FE mesh. The actual *material frame* $\{x_1',x_2',x_3'\}$ follows the material during the deformation. It can be defined as three orthogonal lines initially drawn on the material and which become curve and non Cartesian as the material deforms. This frame is generally unknown in the FEM framework. Finally, the *local frame* $\{x_1,x_2,x_3\}$ is used during FE simulations to describe the material (anisotropic) behavior. This frame is expected to propose the best orthogonal average position of the material frame.

This paper mainly deals with three different approaches regarding the choice of the local reference system used to represent the material's behavior: a method based on the kinematics of the FE formulation, a corotational method and the Mandel spin approach. An experimental validation is examined in order to assess the quality of each approach. As it induces large rotations of local axes, a shear test was investigated during this study.

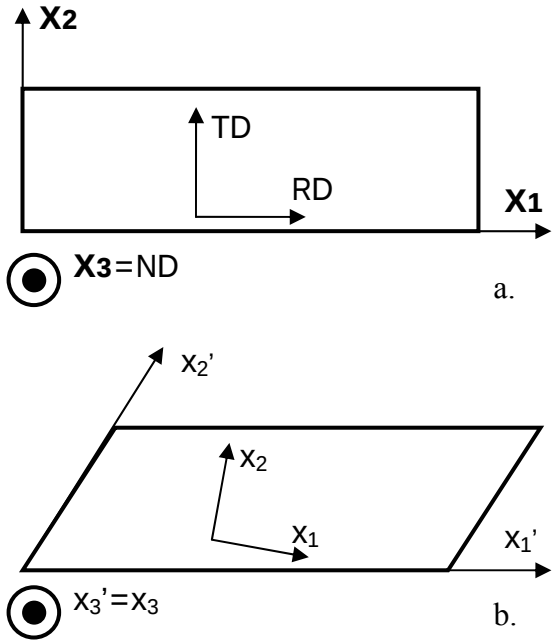

FIGURE 1. Definition of reference frames during shearing in (a.) initial state and (b.) deformed state.

NUMERICAL MODELS

The numerical simulations described in the present paper were achieved thanks to the self-made FE code LAGAMINE [1-2].

Minty constitutive law

For the present study, a crystal plasticity law adapted to macroscopic simulations was used. This law is based on a local yield locus approach able to predict texture evolution during FE modeling of industrial forming processes. With this model, only a small zone of the yield locus is computed. This zone is updated when its position is no longer located in the part of interest in the yield locus or when the yield locus changes due to texture evolution.

This model is specific in the sense that it does not use a yield locus formulation either for plastic criterion or in the stress integration scheme. A linear stress-strain interpolation in the 5-dimensional (5D) stress space is used at the macroscopic scale:

$$\boldsymbol{\sigma} = \tau \mathbf{C}\mathbf{u} \qquad (1)$$

In this equation, $\boldsymbol{\sigma}$ is a 5D vector containing the deviatoric part of the stress; the hydrostatic part being computed according to an isotropic elasticity law. The 5D vector $\mathbf{u}$ is the deviatoric plastic strain rate direction (it is a unit vector). τ is a scalar describing an isotropic work hardening.

The macroscopic anisotropic interpolation is included in the matrix $\mathbf{C}$. Its identification relies on 5 directions: $\mathbf{u}_i$ (i=1…5) advisedly chosen in the deviatoric strain rate space and their associated deviatoric stresses: $\boldsymbol{\sigma}_i$ (i=1…5) computed by the polycrystal plasticity model. This micro-macro model uses Taylor's assumption of equal macroscopic strain rate and microscopic crystal strain rate. It computes the average of the response of a set of representative crystals evaluated with a microscopic model taking into account the plasticity at the level of the slip systems. In this paper, a Full Constraints (FC) Taylor's model coupled with a rate insensitive crystal plastic model is investigated.

The texture evolution is computed using Taylor's model on the basis of the strain history for each integration point at every FE time step. Further details and properties of Minty law can be found in [2].

Local axes definitions

Three different methods for the determination of the local reference frame are proposed hereafter.

The Constant Symmetric Local Velocity Gradient

The *Constant symmetric local velocity gradient* (CSLVG) method used to determine an adequate local reference system was initially developed by Cescotto and Munhoven [3-4]. This method is based on the kinematics of the FE method.

At a first stage, all vectors and tensors are expressed in the global reference system, where the FE mesh is defined. The global reference system remains fixed during the deformation of the solid. The kinematics in continuum mechanics involve the computation of the deformation gradient tensor:

$$\mathbf{F} = \frac{\partial \mathbf{x}}{\partial \mathbf{X}} \qquad (2)$$

where $\mathbf{x} = \mathbf{x}(\mathbf{X}, t)$ is the mapping of the initial configuration of the solid, having coordinates $\mathbf{X}$, to the current configuration at time t. The velocity gradient in the current configuration is computed with equation (3).

$$\mathbf{L} = \frac{\partial \dot{\mathbf{x}}}{\partial \mathbf{x}} = \dot{\mathbf{F}}\mathbf{F}^{-1} \qquad (3)$$

The symmetric part and the skew-symmetric part of $\mathbf{L}$ are respectively the well-known strain rate tensor and the spin tensor, related to rigid body rotation.

The implementation of a non linear constitutive law in a large strain FE code implies a step by step procedure. The integration of the kinematic equations must be achieved carefully due to the incremental procedure.

The configuration at the beginning of one step is called A at time t_A and the configuration at the end of this step is B at time t_B. During the computation of one FE time step, the velocity field at the beginning of the step is known and an estimation of the velocity field at the end of the step is assumed. The deformation gradient tensors at the beginning and the end of the step are computed:

$$\mathbf{F}_A = \frac{\partial \mathbf{x}_A}{\partial \mathbf{X}} \quad \textit{and} \quad \mathbf{F}_B = \frac{\partial \mathbf{x}_B}{\partial \mathbf{X}} \qquad (4)$$

The incremental deformation gradient tensor for the considered step is:

$$\mathbf{F}_{AB} = \mathbf{F}_B \mathbf{F}_A^{-1} = \frac{\partial \mathbf{x}_B}{\partial \mathbf{x}_A} \qquad (5)$$

According to this incremental process, the configurations at the beginning and the end of the step are known but a strain path must be chosen between these two configurations. Different assumptions have been examined by several authors, see e.g. [5-6].

The *constancy* assumption of the velocity gradient (one important feature of the model) imposes the strain path. According to equation (3), the deformation

gradient tensor must satisfy the following differential equation:

$$\mathbf{L} = \dot{\mathbf{F}}(t)\left[\mathbf{F}(t)\right]^{-1} = \textbf{constant}, \quad t \in \left[t_A, t_B\right] \quad (6)$$

with the initial condition:

$$\mathbf{F}(t_A) = \mathbf{F}_A \quad (7)$$

The following solution fulfils equations (6) and (7):

$$\mathbf{F}(t) = \exp\left(\mathbf{L}(t - t_A)\right)\mathbf{F}_A \quad (8)$$

The additional condition $\mathbf{F}(t_B) = \mathbf{F}_B$ allows finding the constant value of the velocity gradient:

$$\mathbf{L} = \frac{1}{\Delta t}\ln\left(\mathbf{F}_{AB}\right) \quad (9)$$

where $\Delta t = t_B - t_A$ is the size of the time step.

The velocity gradient computed with equation (9) is constant during the time step but it is generally non-symmetric as $\mathbf{F}_{AB}$ is not necessary symmetric. The *symmetry* of the velocity gradient can however be obtained by expressing it in another reference system. In other words, the symmetry condition in this method fixes the choice of the local reference system.

Let's now present how to determine the local reference system and the velocity gradient according to the symmetry condition. All vectors and tensors expressed in the local reference system are noted with a $'$.

First, the deformation gradient tensor expressed in the local reference system is obtained thanks to equation (10).

$$\mathbf{F}' = \frac{\partial \mathbf{x}'}{\partial \mathbf{X}'} = \frac{\partial \mathbf{x}'}{\partial \mathbf{x}}\frac{\partial \mathbf{x}}{\partial \mathbf{X}}\frac{\partial \mathbf{X}}{\partial \mathbf{X}'} = \mathbf{R}^T\mathbf{F}\mathbf{R}_0 \quad (10)$$

where $\mathbf{R}$ is the current rotation matrix between the local and the global reference systems (the orthogonal condition of rotation matrices implies $\mathbf{R}^{-1} = \mathbf{R}^T$). $\mathbf{R_0}$ is the corresponding rotation matrix at the beginning of the process.

Due to the step by step procedure of the FE code, the rotation matrix $\mathbf{R}$ has the value $\mathbf{R_A}$ at the beginning of the step and $\mathbf{R_B}$ at the end of the step. Indeed, while the global reference system remains always fixed, the local one evolves during the time step. The incremental rotation of the local reference system during the time step is simply $\mathbf{R}_B\mathbf{R}_A^T$.

Similarly to equation (5), the incremental deformation gradient expressed in the local reference system is:

$$\mathbf{F}'_{AB} = \mathbf{F}'_B\mathbf{F}'^{-1}_A = \frac{\partial \mathbf{x}'_B}{\partial \mathbf{x}'_A} \quad (11)$$

The local velocity gradient can then be obtained:

$$\mathbf{L}' = \frac{1}{\Delta t}\ln\left(\mathbf{F}'_{AB}\right) \quad (12)$$

This velocity gradient is constant during the time step and it is furthermore assumed to be symmetric. Equation (12) then implies that $\mathbf{F}'_{AB}$ is also symmetric.

Making use of equation (10) allows developing the formulation of the local incremental deformation gradient:

$$\begin{aligned}\mathbf{F}'_{AB} &= \mathbf{F}'_B\mathbf{F}'^{-1}_A = \left(\mathbf{R}_B^T\mathbf{F}_B\mathbf{R}_0\right)\left(\mathbf{R}_0^T\mathbf{F}_A^{-1}\mathbf{R}_A\right) \\ &= \mathbf{R}_B^T\mathbf{F}_B\mathbf{F}_A^{-1}\mathbf{R}_A = \mathbf{R}_B^T\mathbf{F}_{AB}\mathbf{R}_A\end{aligned} \quad (13)$$

At this stage, we define

$$\mathbf{F}^*_{AB} \triangleq \mathbf{F}_{AB}\mathbf{R}_A = \mathbf{R}_B\mathbf{F}'_{AB} \quad (14)$$

where the second equality derives from (13).

Finally, equation (12) yields to:

$$\begin{aligned}\mathbf{L}' &= \frac{1}{\Delta t}\ln\left(\mathbf{F}'_{AB}\right) = \frac{1}{2\Delta t}\ln\left(\mathbf{F}'_{AB}\mathbf{F}'_{AB}\right) \\ &= \frac{1}{2\Delta t}\ln\left(\left(\mathbf{F}'_{AB}\right)^T\mathbf{F}'_{AB}\right) \\ &= \frac{1}{2\Delta t}\ln\left(\left(\mathbf{R}_B^T\mathbf{F}^*_{AB}\right)^T\left(\mathbf{R}_B^T\mathbf{F}^*_{AB}\right)\right) \\ &= \frac{1}{2\Delta t}\ln\left(\left(\mathbf{F}^*_{AB}\right)^T\mathbf{R}_B\mathbf{R}_B^T\mathbf{F}^*_{AB}\right) \\ &= \frac{1}{2\Delta t}\ln\left(\left(\mathbf{F}^*_{AB}\right)^T\mathbf{F}^*_{AB}\right)\end{aligned} \quad (15)$$

The symmetry condition of $\mathbf{F}'_{AB}$ has been used in the above developments, while this last formulation of the local velocity gradient is checked to be effectively symmetric.

The implementation of this method in the FE code is achieved according to the following algorithm:

0. All variables at the beginning of the step (state *A*) are known (expressed in the global reference system) according to previous step computations.

1. With the estimation of the velocity field at the end of the step, $\mathbf{F}_{AB}$ is computed according to equations (4) and (5).

2. The definition of $\mathbf{F}^*_{AB}$ is exploited (first equality of equation (14)).

3. The constant symmetric local velocity gradient $\mathbf{L}'$ is computed according to the last equality of equation (15).

4. The stress tensor at the beginning of the step is expressed in the local reference system according to:

$$\boldsymbol{\sigma}'_A = \mathbf{R}_A^T\boldsymbol{\sigma}_A\mathbf{R}_A \quad (16)$$

5. The constitutive law is called to achieve the stress integration on the current time step:

$$\boldsymbol{\sigma}'_B = \boldsymbol{\sigma}'_A + f\left(\boldsymbol{\sigma}'_A, \mathbf{L}', \Delta t, \text{internal variables}\right) \quad (17)$$

Conveniently, the incremental objectivity is automatically satisfied thanks to the computation in the local reference system. As a consequence, no Jaumann type corrections must be added to the natural derivatives during the stress integration.

6. The right decomposition of $\mathbf{F}^*_{AB}$ yields to:

$$\mathbf{F}^*_{AB} = \mathbf{R}^*\mathbf{U}^* \quad (18)$$

Identification of equation (18) and the second equality of equation (14) allows determining $\mathbf{R}_B$. Indeed, bearing in mind that $\mathbf{F}'_{AB}$ is symmetric, we have $\mathbf{R}_B = \mathbf{R}^*$ and incidentally $\mathbf{F}'_{AB} = \mathbf{U}^*$.

7. Finally, the stress tensor at the end of the step can be computed:

$$\boldsymbol{\sigma}_B = \mathbf{R}_B\boldsymbol{\sigma}'_B\mathbf{R}_B^T \quad (19)$$

The corotational method

The second method investigated for the determination of the local reference system is the use of a corotational reference system. This frame is closely linked to the element nodal coordinates. This reference system must have its origin at the center of the element and its reference axes are aligned (as much as possible, depending on the element shape) with element edges. This method has mainly geometrical bases and is easily implemented in a FE code. However, contrarily to the CSLVG method, the corotational method does not guaranty the objectivity of the stress integration. A separate objectivity method (e.g. Jaumann derivatives) must be used.

The Mandel spin method

The corotational approach is based on the geometric configuration of the finite element, while the CSLVG method is based on the kinematics of the element. These two methods are independent of the constitutive law used to model the material behavior.

The Mandel spin approach described here is quite different in the sense that it is linked to the material model and especially to the crystals constituting the studied polycrystal. The macroscopic rotation of the material is computed from the rotation of each crystal.

Due to its cubic symmetry, the crystal lattice must always remain orthogonal. The crystal rotations during plastic straining are therefore defined unquestionably. The problem of the non orthogonal axes $\{x_1', x_2', x_3'\}$ in Figure 1(b.) is avoided if we focus on crystal rotations.

In order to have a representation of the crystal rotations, the Mandel spin approach requires the use of a constitutive law based on texture analysis with computation of the texture evolution during plastic deformations. In LAGAMINE code, the Mandel spin approach must be coupled with Minty constitutive law (described above). The orientation of each crystal lattice of the material's texture representative set is expressed with Euler angles during the whole finite element simulation. The rotation of every crystal during each finite element time step can then be deduced.

The main difficulty during the computation of the Mandel spin is the computation of the macroscopic rotation of the polycrystal from the rotations of all crystals of the representative set. A mean rotation must be computed from crystal rotations.

In the particular case the rotation axis is identical for each crystal, the mean rotation can simply be computed as the mean rotation angle around the common axis.

Unfortunately, in the general three-dimensional case, the rotation axis is different from one crystal to another. Indeed, during numerical shearing simulations, only a few crystals rotate around an axis close to the expected macroscopic rotation axis. The rotation angles are also very different from one crystal to another. The rotation axes of the crystals generally have a small deviation from the macroscopic rotation axis. A typical deviation of around 10° between the macroscopic and the crystal rotation axes was observed. However, some crystals rotate around axes very different from the macroscopic one.

Four techniques were investigated for the computation of the macroscopic mean rotation during one finite element time step. Two techniques use quaternions to represent the crystal rotations and two techniques use skew-symmetric spin tensors. Besides, two averaging techniques were developed. The authors refer to [7] for a detailed description of each technique.

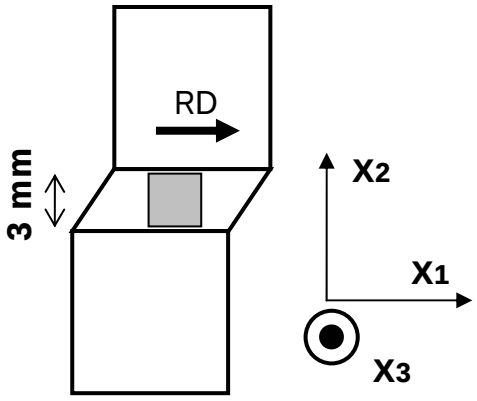

FIGURE 2. Experimental test and sample for texture measurement.

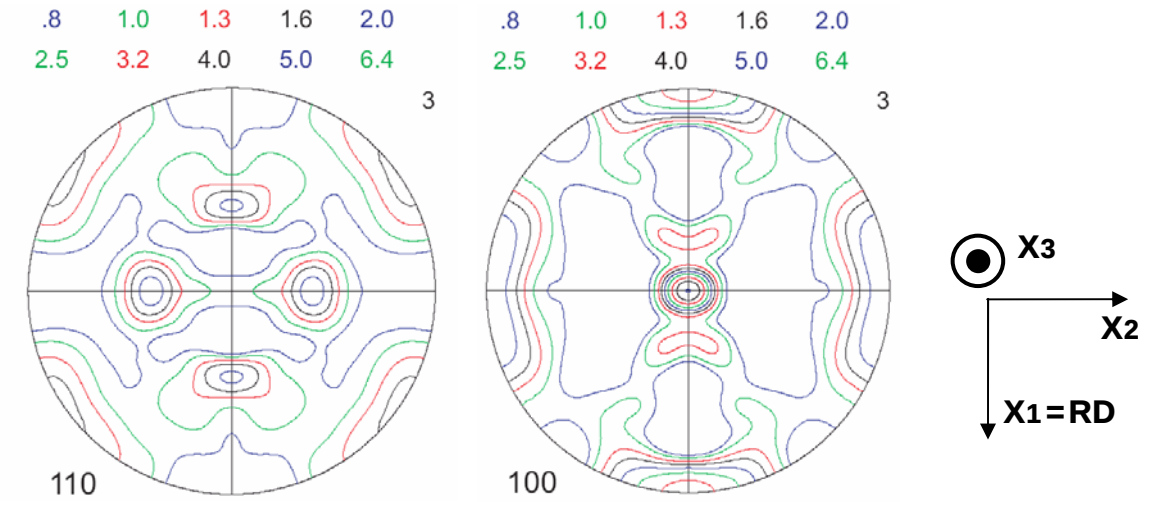

FIGURE 3. Initial texture of AL6016 material in terms of 110 and 100 pole figures.

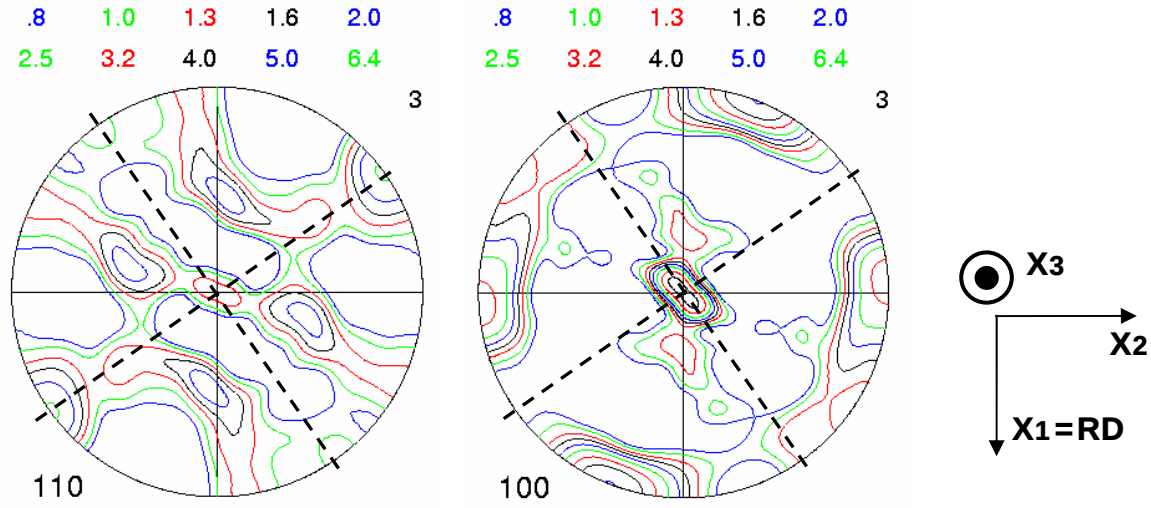

FIGURE 4. 110 and 100 pole figures of the measured texture on the deformed material (shear strain = 0.47).

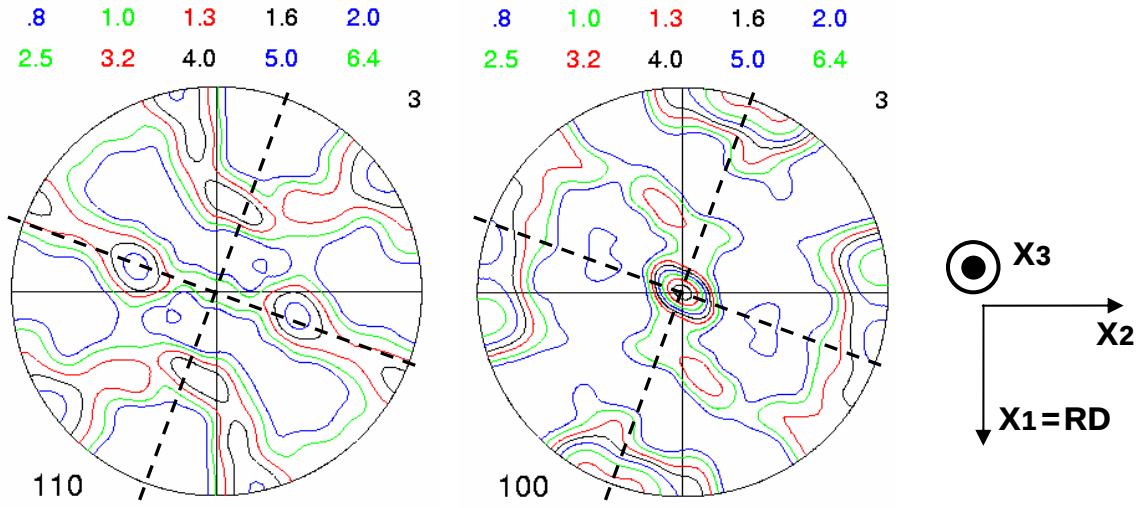

FIGURE 5. Predicted 110 and 100 pole figures after shearing simulation using Minty law.

ALUMINUM SHEET SHEAR TEST

In order to assess the quality of the three different local axes rotation methods proposed above, a simple shear test of aluminum AL6016 sheet was investigated. The sketch of the shear test is presented in Figure 2. The shearing zone of the material was 3mm thick, 30mm long and the thickness of the sheet was 0.94mm. The remaining parts of the sheet were used for clamping. The shearing was conducted up to a shear strain γ of 0.47, which was chosen to be just below the material fracture. Further details about the experimental procedure can be found in [7].

In order to validate the texture predicted by Minty law, a texture measurement on the deformed sample was performed. The zone used for texture measurement was extracted from the sheared zone as shown in Figure 2.

The initial texture of AL6016 is shown in Figure 3. The measured texture on the deformed sample is presented in Figure 4 while the predicted texture appears in Figure 5. A good (quantitative) agreement between experimental and numerical textures is noticeable. In Figures 4 and 5, the new pseudo-orthotropy axes, corresponding to the main symmetry axes of the pole figures are plotted. The orientations of these axes with respect to the initial orthotropy axes are reported in Table 1. As can be seen, even if the two textures are very similar, their symmetry axes are very different. The decision of using these symmetry axes as being adequate local axes is, in this case, quite questionable.

Table 2 presents the rotation angles computed at the end of the shear test for the three investigated methods (the four techniques used for the Mandel spin approach gave very similar results). The three methods are in rather good agreement.

TABLE 1. Rotation of the orthotropy axes.

Texture analyzed	Rotation angle around X3 axis
Measured final texture	+35°
Predicted final texture	-20°

TABLE 2. Rotation of the local reference frame.

Method used	Rotation angle around X3 axis
CSLVG	-13.44°
Corotational	-12.56°
Mandel spin	-12.07°

CONCLUSION

This paper presents three different methods for the computation of the rotation of the local reference frame during FE simulations. For the aluminum sheet shear test, the three methods gave similar results. Contrarily, the analysis of the orthotropy axes of the deformed texture is not (in this case) a good measure of the rotation of the material frame.

The main characteristics of the three rotation methods are:

- The Mandel spin has a physical meaning in term of crystal analysis; hence, it is accurate even for very large strains [7]. On the other hand, it must be linked to a crystal plasticity constitutive law with computation of the texture evolution. As a consequence, it involves large computation time.
- The corotational method is conceptually very simple and its implementation in a FE code is also straightforward. Nevertheless, its results are quite satisfactory. The main drawback of this method is that it does not ensure the objectivity during the FE computation.
- The CSLVG method derives from the kinematics of the FE code. The theoretical developments are not straightforward but its implementation in a FE code is uncomplicated and it is computation time efficient. A major advantage of this method is that it ensures objectivity by making use of a symmetric velocity gradient. However, it generally overestimates the rotation of the local frame especially for very large strains.

ACKNOWLEDGMENTS

The authors thank the Belgian Federal Science Policy Office (Contract P5/08) for their financial support. As Research Director, A.M.H. thanks the Fund for Scientific Research (Belgium) for its support.

REFERENCES

1. A.M. Habraken, J.F. Charles, J. Wegria, S. Cescotto, *Int. J. of Forming Processes* **1**, Issue 1 (1998).
2. A.M. Habraken, L. Duchêne, *Int. J. of Plasticity* **20**, Issue 8-9, 1525-1560 (2004).
3. S. Cescotto, *Finite deformation of solids*. Numerical Modelling of Material Deformation Processes, Hartley P., Pillinger I., Sturgess C. (Eds.), Springer-Verlag, pp. 20-67 (1984).
4. S. Munhoven, A.M. Habraken, *Application of an anisotropic yield locus based on texture to a deep drawing simulation*. In: Proc. Conf. NUMIFORM 95, Balkema, Rotterdam (1995).
5. T.J.R. Hughes, Theoretical foundation for large-scale computations of nonlinear material behaviour. Proc. Workshop on Theor. Foundation for Large-Scale Comput. of Nonlinear Material Behaviour, 29-63 (1983).
6. J.P. Ponthot, *Int. J. of Plasticity* **18**, 91-126 (2002).
7. L. Duchêne, T. Lelotte, P. Flores, S. Bouvier, A.M. Habraken, Rotation of axes for anisotropic metal in FEM simulations, *Int. J. of Plasticity*, to appear.